Molecular Imaging Identifies Regions with Microthromboemboli During Primary Angioplasty in Acute Coronary Thrombosis

Tadamichi Sakuma, MD; Jiri Sklenar, PhD; Howard Leong-Poi, MD; Norman C. Goodman, BSc; David K. Glover, PhD; and Sanjiv Kaul, MD

Cardiovascular Imaging Center and Experimental Cardiology Laboratory, Cardiovascular Division, Department of Medicine, University of Virginia Health System, Charlottesville, Virginia

Microthromboemboli (MTE) may contribute to the no-reflow phenomenon in acute myocardial infarction (AMI) either spontaneously or after primary percutaneous transluminal coronary angioplasty (PTCA). We hypothesized that myocardial MTE in acute coronary syndromes can be identified on imaging by in vivo ^{99m}Tc labeling of the coronary thrombus with a compound that binds to the glycoprotein IIb/IIIa present on activated platelets (DMP-444). **Methods:** Fifteen dogs underwent left anterior descending coronary artery (LAD) injury in to produce thrombus, whereas 5 control dogs had LAD ligation. Before recanalization, the risk area (RA) and myocardial blood flow (MBF) were measured, and in vivo thrombus labeling was performed using ^{99m}Tc-labeled DMP-444. Nine of the 15 LAD injury dogs had occlusive thrombus on angiography and underwent PTCA. MBF measurements were repeated 30 and 60 min after recanalization, and ^{99m}Tc autoradiography (hot spot imaging) was performed ex vivo to determine the extent and magnitude of MTE. **Results:** The ratio of hot spot size to RA size was higher in the 9 LAD injury dogs with thrombus compared with the 6 dogs with no thrombus (90% ± 22% vs. 42% ± 16%; $P = 0.005$). In control dogs, this ratio was significantly lower (29% ± 11%; $P = 0.05$). ^{99m}Tc activity within the RA was higher in 8 of the 15 coronary injury dogs with AMI compared with those without AMI (1.8 ± 0.48 vs. 1.24 ± 0.22; $P = 0.02$). **Conclusion:** MTE can be detected and quantified after primary PTCA. The infarct size is proportional to the magnitude and extent of MTE, indicating that MTE may contribute to the AMI. Thus, in vivo thrombus labeling during reperfusion may provide important information in patients with AMI that may lead to better adjuvant therapy during PTCA.

Key Words: glycoprotein IIb/IIIa receptor; myocardial blood flow; autoradiography

J Nucl Med 2004; 45:1194–1200

Primary percutaneous transluminal coronary angioplasty (PTCA) is a well-established treatment option in patients with acute coronary thrombosis. However, the procedure itself may dislodge the thrombus in whole or in part, resulting in distal microthromboembolization (MTE) that, in turn, could cause ventricular arrhythmias, contractile dysfunction, infarctlets, and reduced coronary flow reserve (*1*,*2*). It may also contribute to the overall infarct size (IS). An assessment of the degree and extent of MTE after primary PTCA could therefore assist in determining the short-term outcome as well as adjuvant therapy. In this study, we hypothesized that MTE after primary PTCA can be identified on imaging by in vivo labeling of the coronary thrombus with a compound that binds to the glycoprotein IIb/IIIa present on activated platelets (*3*,*4*). We also sought to investigate whether the IS after reperfusion is related to MTE.

MATERIALS AND METHODS

Animal Preparation and Experimental Protocol

In the past, models of acute myocardial infarction (AMI) have generally used coronary ligation to produce coronary occlusion (*5*–*9*). In the clinical setting, however, sudden coronary occlusion is most often associated with coronary thrombosis. We have developed a model of acute coronary thrombosis in dogs (*10*) that we used for this study, which was approved by the Animal Research Committee at the University of Virginia and conformed to the position of the American Heart Association on Research Animal Use. Twenty adult mongrel dogs were anesthetized with 30 mg·kg^{-1} of sodium pentobarbital and mechanically ventilated with a respirator pump. An 8-French catheter sheath was placed in the left carotid artery for coronary angiography and PTCA. Similar catheters were placed in both femoral arteries for duplicate reference sample withdrawal during radiolabeled microsphere injection for measuring regional myocardial blood flow (MBF), and one of them was connected to a multichannel recorder for arterial pressure monitoring. Catheters were placed in both femoral veins for administration of fluids and infusion of microbubbles. A heated mattress was used to maintain the core body temperature at 38°C.

A left lateral thoracotomy was performed and the heart was suspended in a pericardial cradle. A 6-French catheter was placed in the left atrium for injection of radiolabeled microspheres. MBF measurements and coronary angiography were performed at baseline (Fig. 1). The mid and distal portions of the left anterior descending coronary artery (LAD) were then dissected free from surrounding tissues. In 15 dogs, a PTCA balloon (3.0-mm diam-

Received Sep. 30, 2003; revision accepted Feb. 3, 2004.

For correspondence or reprints contact: Sanjiv Kaul, MD, Cardiovascular Division; Box 800158, Medical Center, University of Virginia, Charlottesville, VA 22908-0158.

E-mail: sk@virginia.edu

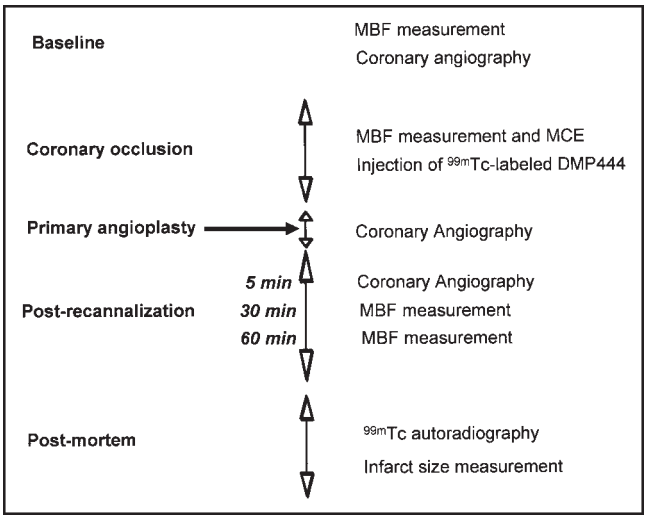

FIGURE 1. Time-line diagram of sequence of experimental procedures.

eter, 9.0-mm length) was advanced into the LAD over a guide wire. Umbilical tape was tightened around the distal LAD, and the mid-LAD was subjected to external injury using forceps. Balloon inflation was started at 6–8 atmospheric pressure 20 mm proximal to the distal ligation site for 50–200 min (mean, 110 min). The different occlusion times were used to create thrombi of different sizes.

In 5 control dogs, the LAD was occluded for approximately 150 min by tightening an umbilical tape around it without producing a coronary thrombus. These dogs were used since microthrombi can occur within the ischemic myocardium even in the absence of coronary thrombosis because of local glycoprotein IIb/IIIa and $\alpha_v\beta_3$ activation (*11–13*).

Just before recannalization, myocardial contrast echocardiography (MCE) was performed to measure the risk area (RA) and radiolabeled microspheres were injected for measurement of MBF. ^{99m}Tc-DMP-444 was administrated intravenously for in vivo labeling of the coronary thrombus (Fig. 1). Thereafter, the LAD ligation was reversed and PTCA was performed in the LAD injury dogs if an occlusive thrombus was seen on coronary angiography. MBF as well as hemodynamic data were measured at both 30 and 60 min after successful recanalization in all dogs. We chose these 2 times after reperfusion because we have previously shown that MTE can spontaneously dissolve between these times after reperfusion (*10*) and we wanted to study the effect of the magnitude of MTE on the spontaneous resolution of no reflow. At the end of the experiment, sutures were placed on the myocardium at the level of the ultrasound transducer to identify the MCE imaging plane postmortem. The dogs were then killed with a solution of pentobarbital and potassium and the heart was removed. The slice corresponding to the MCE plane was then cut for ^{99m}Tc autoradiography, IS measurement, and radiolabeled microsphere-derived MBF determination (Fig. 1). Using a single heart slice we were able to register all datasets accurately.

Thrombus Imaging

In vivo labeling of the coronary thrombus was achieved by intravenous administration of 37 MBq·kg^{-1} of ^{99m}Tc-labeled DMP-444 (DuPont Pharmaceuticals). This agent binds to the glycoprotein IIb/IIIa platelet receptor, allowing imaging of the thrombus (*3*). It is a hydrazinenicotinamide-functionalized compound (cyclo[D-Val-NmeArg-Gly-Asp-Mamb(5(6-(6-hydrazinonicotinamido)hexamide))] [HYNICitide]) labeled with ^{99m}Tc using tricine and a water-soluble phosphine as coligands. Its 50% inhibitory concentration for the IIb/IIIa receptor is 11 nmol/L·L^{-1} (*4*).

At the end of the experiment, the heart slice corresponding to the MCE image was placed directly on the collimator of a γ-camera (Orbiter 37; Siemens). A high-resolution collimator with a 140-keV, 20% window centered around the photopeak of ^{99m}Tc with a 128 × 128 matrix was used. Image quantification was performed on a nuclear medicine computer (ICON; Siemens) (*14*).

For quantification of regional myocardial ^{99m}Tc activity, regions of interest were drawn over the background-subtracted RA and the normal contralateral wall, and the average activity in these regions were measured. A count ratio was computed by dividing the average counts per pixel in the RA by the average counts per pixel in the contralateral wall. The hot spot was defined as the region with more than the mean + 2 SD of the activity in the normal myocardium (as defined by MCE) and was planimetered and expressed as a percentage of the left ventricular (LV) short-axis area.

MBF Measurements

MBF was measured with left atrial injections of $2{\cdot}10^6$, 11-μm radiolabeled microspheres (DuPont Medical Products) suspended in 4 mL of 0.9% saline and 0.01% Tween-80 (*15*). The microspheres, their energy windows, and half-lives are as follows: ^{113}Sn, 340–440 keV, 115 d; ^{103}Ru, 450–550 keV, 39 d; and ^{46}Sc, 842–1,300 keV, 84 d. None of these isotopes has kiloelectron volts in the range of that of ^{99m}Tc. Duplicate reference blood samples (10 mL each) were withdrawn from the femoral arteries over 130 s with a constant-rate withdrawal pump (model 944; Harvard Apparatus). After autoradiography, the LV short-axis slice corresponding to the MCE image was cut into 16 wedge-shaped pieces, excluding the papillary muscles, and each piece was further divided into epicardial, midmyocardial, and endocardial segments. The tissue and reference blood samples were counted 1 wk later in a well counter with a multichannel analyzer to allow for complete decay of ^{99m}Tc. Corrections were made for activity spilling from one energy window to another with a custom-designed program (*14*).

MBF to each segment was calculated using the equation Qm = (Cm·Qr)·Cr, where Qm is blood flow to the myocardial segment (mL·min^{-1}), Cm is tissue counts, Qr is rate of arterial sample withdrawal (mL·min^{-1}), and Cr is arterial reference sample counts (*15*). The absolute MBF (mL·min^{-1}·g^{-1}) to each of the 48 pieces was calculated as the quotient of the flows and the weight of the segment.

MBF in each segment within the LAD was also represented with a parametric image with color coding to display the magnitude of MBF. This custom-designed program uses colors ranging from brown (low flow) to bright yellow (high flow) (*16*). No reflow was defined when the ratio of endocardial MBF in the center of the RA and MBF in the normal myocardium (defined by MCE)$^{-1}$ (MBF ratio) was <0.25 at both 30 and 60 min after recanalization. This criterion was used because it has been previously shown that no reflow and necrosis are closely correlated and that they are seen only when MBF < 25% of normal (*6–9,17,18*).

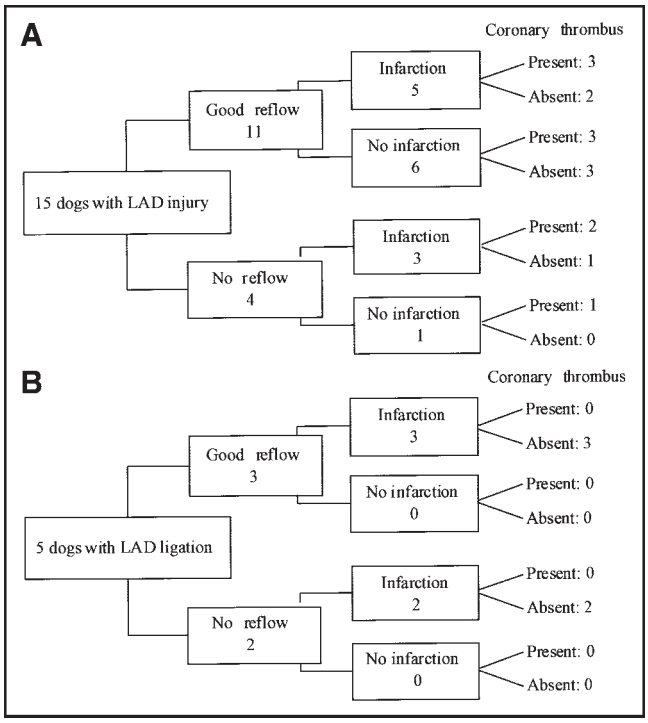

FIGURE 2. Breakdown of LAD injury (A) and LAD occlusion (B) dogs based on tissue perfusion and presence or absence of necrosis.

RA Measurement

RA was measured during coronary occlusion using MCE. Intermittent harmonic imaging was performed using a phased-array system (Power Vision 6000; Toshiba) with a transducer that transmits ultrasound at a mean frequency of 2.1 MHz and receives 4.2 MHz. Six end-systolic images were obtained at a pulsing interval of 10 cardiac cycles during a continuous infusion of 2 mL of Definity (Bristol Myers Squibb Medical Imaging) diluted in 23 mL of 0.9% saline.

Images were aligned using computer cross-correlation as previously described (*16–18*). Color coding was applied to background-subtracted images to visually enhance regional differences in myocardial contrast enhancement (*16–18*). The RA was planimetered by an observer who was unaware of the region with no contrast enhancement and was expressed as a percentage of the LV short-axis slice as previously described (*16–18*). We and others have validated this method of RA assessment against postmortem techniques (*17–20*).

IS Determination

At the end of the experiment, the heart was excised, and a 1-cm slice corresponding to the MCE imaging plane was immersed in a solution of 1.3% 2,3,5-triphenyltetrazolium chloride (SigmaCorp.) and 0.2 mol/L Sorensen's buffer in distilled water (pH 7.4) at 37°C for 20 min, followed by fixation in 10% formalin (*21*). The apical and basal sides of the stained specimen were imaged with a digital scanning camera. The regions with unstained myocardium on both aspects of the slice was measured by planimetry and averaged. Infarct size was determined as a percentage of the LV short-axis area.

Statistical Methods

Results are expressed as mean ± 1 SD. Data were compared using the Mann–Whitney *U* test and correlations were assessed using by the Pearson correlation coefficient. Receiver operating characteristic (ROC) curves were generated to determine the best cutoff for predicting AMI using the ^{99m}Tc count ratio. All findings were considered significant at $P < 0.05$ (2-sided).

RESULTS

On coronary angiography, an occlusive thrombus was observed in 9 of the 15 dogs undergoing LAD injury and no detectable thrombus was noted in 6 dogs. As expected, the coronary occlusion time was significantly longer in the dogs with thrombus compared with those without thrombus (125 ± 45 min vs. 78 ± 25 min; $P = 0.04$). All 9 thrombus dogs underwent successful PTCA. In the 6 dogs without an occlusive thrombus, the PTCA balloon was advanced beyond the site of injury to remove any undetected thrombus. TIMI (Thrombosis in Myocardial Infarction) grade 3 flow was confirmed on repeated angiography in all 15 dogs.

Figure 2A shows the breakdown of the dogs according to MBF and the occurrence of AMI. Only 11 of the 15 LAD injury dogs showed good reflow by MBF measurements, whereas 4 exhibited no reflow. Five of the 11 dogs with good reflow had AMI on tissue staining, whereas 6 did not. In comparison, 3 of the 4 dogs with no reflow had AMI. One dog without AMI exhibited transient no reflow. TIMI grade 3 flow was seen in all control dogs undergoing coronary ligation (Fig. 2B). The duration of coronary occlusion in these dogs was greater than in the LAD injury dogs (161 ± 4 min; $P = 0.02$). Although only 2 dogs showed no reflow, all 5 had AMI.

There was no correlation between coronary occlusion time and hot spot size normalized to RA size in all 20

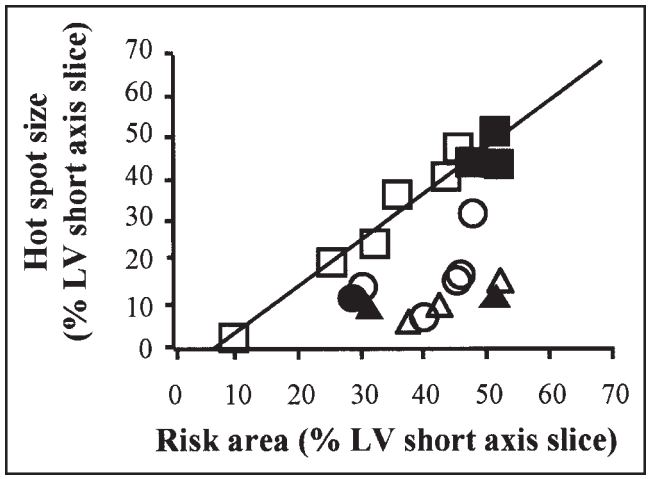

FIGURE 3. Relationship between RA size and hot spot size. ■ and □, LAD injury dogs with thrombus seen on angiography. ● and ○, LAD injury dogs with no thrombus on angiography. ▲ and △, Control dogs with LAD ligation. □, ○, and △, Good reflow. ■, ●, and ▲, No reflow.

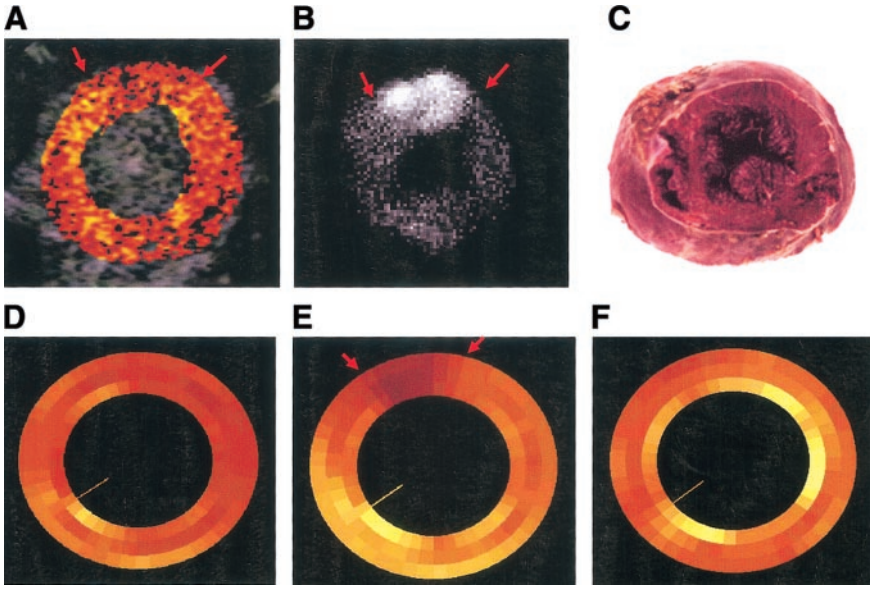

FIGURE 4. Example of adequate reflow and no AMI. Hot spot size (A) corresponded to RA size (B), both shown by arrows. However, there was no infarction (C). Serial changes of MBF are shown at baseline (D), during occlusion (E), and 30 min after recanalization (F).

dogs ($r = 0.07$; $P = 0.80$). The ratio of hot spot to RA size was significantly higher in the 9 LAD injury dogs with thrombus detected on angiography compared with the 6 dogs with no thrombus (90% ± 22% vs. 42% ± 16%; $P = 0.005$). Despite a longer duration of coronary occlusion, this ratio was significantly lower in the control dogs compared with the LAD injury dogs (29% ± 11%; $P = 0.05$). Furthermore, whereas the RA in the control dogs was similar to that of the LAD injury dogs (42% ± 11% vs. 39% ± 12% of the LV short-axis slice; $P = 0.40$), the hot spot size was significantly smaller, 12% ± 4% ($P = 0.05$).

^{99m}Tc activity within the RA was significantly higher in 8 of the 15 dogs with AMI compared with those without AMI (1.8 ± 0.48 vs. 1.24 ± 0.22; $P = 0.02$). Whereas a fair relationship ($r = 0.45$; $P = 0.04$) between MCE-defined RA and the hot spot size on ^{99m}Tc autoradiography was found when all 20 dogs were analyzed (Fig. 3), the relationship improved significantly ($r = 0.97$; $P < 0.0001$) when only the 9 dogs with thrombus seen on angiography were considered. As expected, ^{99m}Tc activity was localized to regions with reduced MBF (<0.25 compared with the normal bed). However, in these regions, no relationship ($r = 0.14$) was found between MBF and ^{99m}Tc activity, indicating that ^{99m}Tc activity was not related to the magnitude of reduced MBF. A positive correlation was noted between the intensity and the size of the hot spot in both the no-reflow and the good reflow dogs ($P = 0.01$ and $P = 0.06$, respectively).

Figure 4 illustrates an example of good reflow without

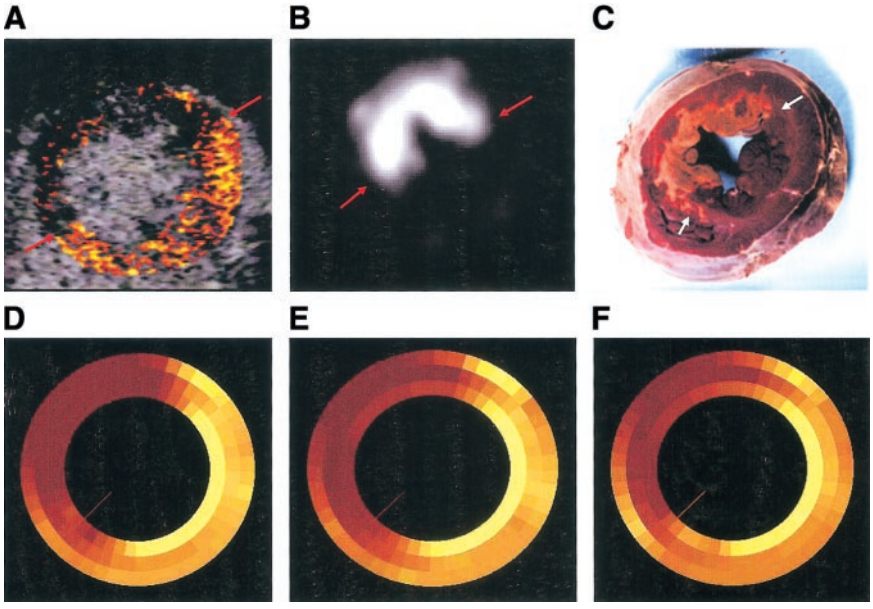

FIGURE 5. Example of no reflow and sizeable AMI (arrows). RA size (A) was similar to hot spot size (B) (arrows). (C) Higher activity of ^{99m}Tc was localized in necrotic area. MBF abnormalities persisted during coronary occlusion (D) as well as at 30 min (E) and 60 min (F) after recanalization.

TABLE 1
MBF in LAD Injury Dogs

MBF	Baseline	Coronary occlusion	After reperfusion	
			30 min	60 min
mL · min^{-1} · g^{-1}	0.93 ± 0.14	0.12 ± 0.02	1.34 ± 0.23	1.54 ± 0.28
Normalized*	1.02 ± 0.12	0.10 ± 0.02	0.65 ± 0.18	0.78 ± 0.20

*Normalized to the opposite normal wall.
Data are expressed as mean ± SEM.

AMI in 1 LAD injury dog. In this example, the hot spot on ^{99m}Tc autoradiography was similar in size with that of the MCE-derived RA. As previously noted (*13*), abnormalities in MBF immediately after reperfusion resolved over time. Depicted in Figure 5 is an example of no reflow with an AMI in 1 LAD injury dog, where high ^{99m}Tc activity was detected within the RA, with the highest counts noted within the necrotic area. MBF abnormalities persisted in this dog during the duration of reperfusion. Tables 1 and 2 depict MBF values from the LAD injury dogs as well as the control dogs, respectively. Actual values and values normalized to the normal wall are given.

Figure 6 represents ^{99m}Tc activity in regions without (n = 18) and with (n = 11) necrosis from the LAD injury dogs as well as similar regions (5 each) from control dogs. The ROC curve generated from these data indicated that the best ^{99m}Tc count ratio cutoff point to separate necrotic from nonnecrotic tissue is 1.36. Using this value, the sensitivity and specificity for predicting AMI were 91% and 94%, respectively (Fig. 7).

DISCUSSION

The new findings in this study are that MTE within the myocardium can be imaged after PTCA in a model of acute coronary thrombosis by administration of ^{99m}Tc-labeled DMP-444 before the procedure. This study also shows that MTE occurring in conjunction with primary PTCA can contribute to the no-reflow phenomenon as well as the IS. Thus, myocardial imaging after in vivo labeling of coronary thrombus with ^{99m}Tc-labeled DMP-444 before attempted reperfusion may provide both diagnostic and prognostic information in patients undergoing primary PTCA. Consequently, pharmacologic and mechanical interventions that reduce the amount of MTE may be beneficial to patients with AMI undergoing PTCA. The effects of these interventions could also be studied using the techniques described in this article.

Critique of Methods

Since we were using a ^{99m}Tc-labeled compound for assessing the degree of MTE, we could not use a similar compound for the assessment of RA. It is for this reason that we used MCE to define RA. This in vivo technique has been well validated for this purpose (*17–20*) and has a higher spatial resolution for defining RA than radiolabeled microsphere–derived MBF.

Platelet activation or plugging can occur locally within the RA even in the absence of MTE. Furthermore, $\alpha_v\beta_3$ activity in platelets as well as the vascular endothelium is also upregulated during ischemia, and an agent that binds to the IIb/IIIa receptor may also cross-react with the $\alpha_v\beta_3$ receptor (*11–13*). It is for this reason that we used control dogs undergoing coronary ligation without thrombus production. Though these dogs also showed the presence of activated IIb/IIIa in the RA, the magnitude and spatial extent of the signal was much less than that of the dogs with vascular injury. As expected, the activity was the greatest in dogs who demonstrated a thrombus on coronary angiography.

We performed quantitative ^{99m}Tc autoradiography by directly placing the heart slice on the collimator of a γ-camera rather than using film. In this manner, our count ratios were accurate. The minimal loss in spatial resolution was not a major concern because of the large differences in the spatial

TABLE 2
MBF in Coronary Ligation (Control) Dogs

MBF	Baseline	Coronary occlusion	After reperfusion	
			30 min	60 min
mL · min^{-1} · g^{-1}	0.95 ± 0.16	0.13 ± 0.03	1.88 ± 0.23	1.74 ± 0.26
Normalized*	1.06 ± 0.15	0.11 ± 0.02	0.89 ± 0.19	0.82 ± 0.17

*Normalized to opposite normal wall.
Data are expressed as mean ± SEM.

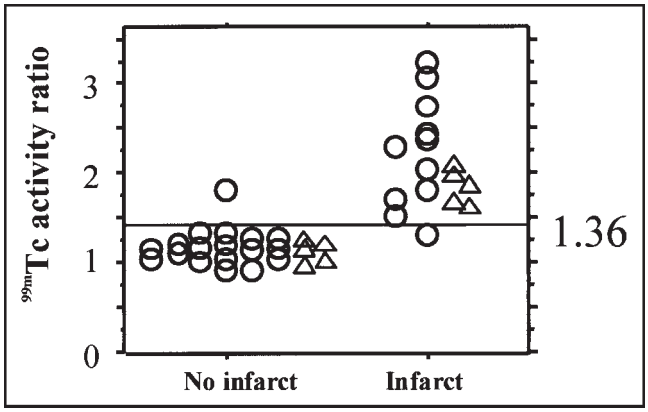

FIGURE 6. ^{99m}Tc activity from regions within RA exhibiting necrosis and no necrosis. ○, ^{99m}Tc activity in LAD injury dogs. △, ^{99m}Tc activity in control dogs.

extent of MTE between the groups. We used a single heart slice over which the ultrasound transducer was fixed during MCE and which was then used for autoradiography, determining IS, and MBF measurements.

A limitation of the study was that we did not use histopathology to confirm the presence of microthrombi in areas with DMP-444 activity. However, this has been validated by others previously (*3,4*). Another limitation is that we did not study a model of atherosclerosis in which a residual coronary stenosis could have been present, potentially requiring stent placement.

Clinical Implications

These results have an important bearing on the understanding of the relationship between no reflow and necrosis because of the controversy regarding the temporal relationship between microvascular abnormalities and myocyte injury. The conventional wisdom is that the microvascular phenomenon is a consequence of cell death (*22*). This belief is based on animal models of coronary ligation and not thrombosis. Studies using MCE in patients with AMI have reported that the low-reflow phenomenon can be partially reversed by the administration of verapamil and nicorandil and that this reversal is associated with improved regional function and outcome (*23,24*). Taken together with the results of our study, it appears that in the setting of coronary thrombosis, part of the no reflow may be caused by MTE and may precede necrosis unless MTE is treated.

Thus, our results imply that measures aimed at reducing the thrombus burden may reduce MTE and IS. These measures could include mechanical means of preventing thrombus from migrating distally and pharmacologic measures directed toward attenuating platelet activation. For instance, a recent study showed that intracoronary thrombectomy with the X-sizer catheter system improved epicardial flow and accelerated ST-segment resolution in patients with acute coronary syndrome (*25*). Improved TIMI grade flow has also been reported in patients with AMI receiving IIb/IIIa receptor antagonists (*26*). In an experimental model of coronary thrombosis and PTCA, we have recently shown that the combined blockade of IIb/IIIa and $\alpha_v\beta_3$ reduced IS substantially (*27*). Molecular imaging of MTE may play a role in clinical trials designed to study such approaches in patients with acute coronary syndromes.

CONCLUSION

Myocardial MTE can be imaged after PTCA in a model of acute coronary thrombosis by administration of ^{99m}Tc-labeled DMP-444 before the procedure. MTE occurring in conjunction with primary PTCA can contribute to the no-reflow phenomenon as well as IS. Thus, myocardial imaging after in vivo labeling of coronary thrombus with ^{99m}Tc-labeled DMP-444 before attempted reperfusion may provide both diagnostic and prognostic information in patients undergoing primary PTCA.

ACKNOWLEDGMENTS

This research was supported in part by the National Institutes of Health (grant 3RO1-HL-48890) and by a fellowship training grant from the Heart and Stroke Foundation of Canada and the Canadian Heart Association, Ottawa, Canada. Dupont Medical Products (Wilmington, DE) provided the radiolabeled microspheres, ultrasound contrast agent, and partial support for postdoctoral training. Toshiba Medical (Nasu, Japan) provided the ultrasound system. Part of this work was presented at the 74th Annual Scientific Session of the American Heart Association, November 11–14, 2001, Anaheim, CA.

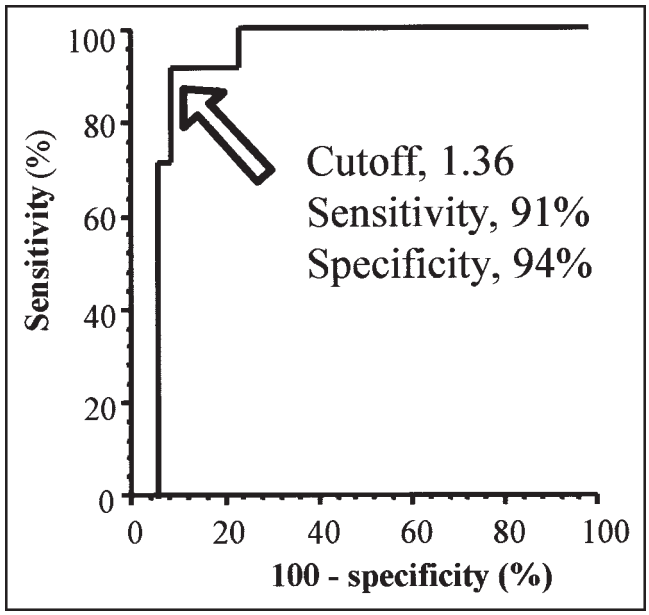

FIGURE 7. ROC curve shows that best cutoff in ^{99m}Tc activity ratio (arrow) is 1.36 for predicting AMI.

REFERENCES

1. Knight CJ. New insights into the pathophysiology of acute coronary occlusion. *Eur Heart J.* 1999;1(suppl F):F1–F6.
2. Heusch G, Schulz R, Baumgart D, et al. Coronary microembolization. *Prog Cardiovasc Dis.* 2001;44:217–230.
3. Mitchel J, Waters D, Lai T, et al. Identification of coronary thrombus with a IIb/IIIa platelet inhibitor radiopharmaceutical, technetium-99m DMP-444: a canine model. *Circulation.* 2000;101:1643–1646.
4. Oyen WJ, Boerman OC, Brouwers FM, et al. Scintigraphic detection of acute experimental endocarditis with the technetium-99m labeled glycoprotein IIb/IIIa receptor antagonist DMP444. *Eur J Nucl Med.* 2000;27:392–399.
5. Reimer KA, Jennings RB. The "wavefront phenomenon" of myocardial ischemic cell death. II. Transmural progression of necrosis within the framework of ischemic bed size (myocardium at risk) and collateral flow. *Lab Invest.* 1979;40: 633–644.
6. Kloner RA, Ganote CE, Jennings RB. The "no-reflow" phenomenon after temporary coronary occlusion in the dog. *J Clin Invest.* 1974;54:1496–1508.
7. Cobb FR, Bache RJ, Rivas F, Greenfield JC. Local effects of acute cellular injury on regional myocardial blood flow. *J Clin Invest.* 1976;57:1359–1368.
8. Johnson WB, Malone SA, Pantely GA, Anselone CG, Bristow JD. No reflow and extent of infarction during maximal vasodilation in the porcine heart. *Circulation.* 1988;78:462–472.
9. Vanhaecke J, Flameng W, Borgers M, Jang I, Van de Werf F, De Geest H. Evidence for decreased coronary flow reserve in viable postischemic myocardium. *Circ Res.* 1990;67:1201–1210.
10. Sakuma T, Leong-Poi H, Fisher NG, et al. Further insights into the 'no-reflow' phenomenon after primary angioplasty in acute myocardial infarction: the role of microthromboemboli. *J Am Soc Echocardiogr.* 2003;16:15–21.
11. Okada Y, Copeland BR, Hamann GF, et al. Integrin $\alpha_v\beta_3$ is expressed in selected microvessels after focal cerebral ischemia. *Am J Pathol.* 1996;149:37–44.
12. Gawaz M, Neumann FJ, Dickfeld T, et al. A vitronectin receptor ($\alpha_v\beta_3$) mediates platelet adhesion to the luminal aspect of endothelial cells: implications for reperfusion in acute myocardial infarction. *Circulation.* 1997;96:1809–1818.
13. Byzova TV, Plow EF. Activation of $\alpha_V\beta_3$ on vascular cells controls recognition of prothrombin. *J Cell Biol.* 1998;143:2081–2092.
14. Petruzella FD, Ruiz M, Katsiyiannis P, et al. Optimal timing for initial and redistribution technetium 99m-N-NOET image acquisition. *J Nucl Cardiol.* 2000; 7:123–131.
15. Heyman MA, Payne BD, Hoffman JI, et al. Blood flow measurements with radionuclide-labeled microshperes. *Prog Cardiovasc Dis.* 1977;20:52–79.
16. Linka AZ, Sklenar J, Wei K, et al. Assessment of transmural distribution of myocardial perfusion with contrast echocardiography. *Circulation.* 1998;98: 1912–1920.
17. Villanueva FS, Glasheen WP, Sklenar J, Kaul S. Characterization of spatial patterns of flow within the reperfused myocardium by myocardial contrast echocardiography: implications in determining extent of myocardial salvage. *Circulation.* 1993;88:2596–2606.
18. Villanueva FS, Camarano G, Ismail S, Goodman NC, Sklenar J, Kaul S. Coronary reserve abnormalities in the infarcted myocardium: assessment of myocardial viability immediately versus late after reflow by contrast echocardiography. *Circulation.* 1996;94:748–754.
19. Firschke C, Lindner JR, Wei K, et al. Myocardial perfusion imaging in the setting of coronary artery stenosis and acute myocardial infarction using venous injection of FS-069, a second generation echocardiographic contrast agent. *Circulation.* 1997;96:959–967.
20. Grayburn PA, Erickson JM, Escobar J, Womack L, Velasco CE. Peripheral intravenous myocardial contrast echocardiography using a 2% dodecafluoropentane emulsion: identification of myocardial risk area and infarct size in the canine model of ischemia. *J Am Coll Cardiol.* 1995;26:1340–1347.
21. Fishbein MC, Meerbaum S, Rit J, et al. Early phase acute myocardial infarct size quantification: validation of the triphenyl tetrazolium chloride tissue enzyme staining technique. *Am Heart J.* 1981;101:593–600.
22. Kloner RA, Rude RE, Carlson N, Maroko PR, DeBoer LW, Braunwald E. Ultrastructural evidence of microvascular damage and myocardial cell injury after coronary artery occlusion: which comes first? *Circulation.* 1980;62:945–952.
23. Taniyama Y, Ito H, Iwakura K, Masuyama T, et al. Beneficial effect of intracoronary verapamil on microvascular and myocardial salvage in patients with acute myocardial infarction. *J Am Coll Cardiol.* 1997;30:1193–1199.
24. Ito H, Taniyama Y, Iwakura K, et al. Intravenous nicorandil can preserve microvascular integrity and myocardial viability in patients with reperfused anterior wall myocardial infarction. *J Am Coll Cardiol.* 1999;33:654–660.
25. Beran G, Lang I, Schreiber W, et al. Intracoronary thrombectomy with the X-sizer catheter system improves epicardial flow and accelerates ST-segment resolution in patients with acute coronary syndrome: a prospective, randomized, controlled study. *Circulation.* 2002;105:2355–2360.
26. de Lemos JA, Antman EM, Gibson CM, et al. Abciximab improves both epicardial flow and myocardial reperfusion in ST-elevation myocardial infarction: observations from the TIMI 14 trial. *Circulation.* 2000;101:239–243.
27. Sakuma T, Sari A, Goodman NC, Lindner JR, Klibanov A, Kaul S. Simultaneous $\alpha_v\beta_3$ and IIb/IIIa inhibition causes a marked reduction in infarct size following reperfusion in a model of acute coronary thrombosis. *J Am Coll Cardiol.* In press.